

Wave packet propagation study of the charge transfer interaction in the $F^- - Cu(111)$ and $- Ag(111)$ systems

A.G. Borisov, J.P. Gauyacq

*Laboratoire des Collisions Atomiques et Moléculaires,
Unité mixte de recherche CNRS-Université Paris-Sud UMR 8625,
Bâtiment 351, Université Paris-Sud, 91405 Orsay CEDEX, France*

S.V. Shabanov

*Department of Mathematics, University of Florida, Little Hall 358,
Gainesville, FL 32611, USA*

Abstract

The electron transfer between an F^- ion and $Cu(111)$ and $Ag(111)$ surfaces is studied by the wave packet propagation method in order to determine specifics of the charge transfer interaction between the negative ion and the metal surface due to the projected band gap. A new modeling of the F^- ion is developed that allows one to take into account the six quasi-equivalent electrons of F^- which are *a priori* active in the charge transfer process. The new model invokes methods of constrained quantum dynamics. The six-electron problem is transformed to two one-electron problems linked via a constraint. The projection method is used to develop a wave packet propagation subject to the modeling constraint. The characteristics (energy and width) of the ion F^- ion level interacting with the two surfaces are determined and discussed in connection with the surface projected band gap.

I. INTRODUCTION

When an atom or a molecule is close to a surface of a solid, its electrons interact with those of the solid, leading to the possibility of an electron transfer between the atom (molecule) and the solid. This charge transfer process plays a very important role in a variety of different situations. In particular, it often occurs as an intermediate step in reactions at surfaces (desorption, fragmentation of adsorbates, chemical reactions, quenching of metastable species, etc.) [1–4]. The one-electron transfer between energetically degenerate electronic levels of the atom and the solid is called the Resonant Charge Transfer (RCT) process. It is usually considered as the most efficient one among various possible charge transfer interactions. Since a few years the development of accurate theoretical approaches to the RCT in the case of free electron metal surfaces [5–11] has led to a successful description of a one-electron transfer in the interaction of ions (atoms) with such surfaces [12–14]. All these approaches are based on the description of single electron being transferred between the atom and the surface. As an example, one can mention the neutralisation of an alkali positive ion by RCT, even if the possibility of capturing the electron in two different spin states somewhat alters the one-electron picture [15,16]. However, many atoms or molecules contain more than one electron which can possibly participate in the charge transfer process, especially, when the active electrons occupy the same energy level. The latter has to be taken into account in any quantitative approach to the RCT [12–17].

For instance, a free fluorine negative ion can be described as a closed $2p^6$ outer electronic shell with six equivalent electrons, and all of them can participate in the RCT when the ion is close to a metal surface. The effects of each electron cannot be simply added up to get a total effect. Indeed, consider the loss of an electron by the ion. Any of the six electrons can be the one that is detached. However, the detachment of one electron *a priori* precludes the detachment of another one. Clearly, the loss of a second electron would be a completely different process because it corresponds to a formation of a positive fluorine ion and, hence, has a different energetics. Such correlations between the outer-shell electrons of the F^-

ion must be accounted for in any description of the RCT. In this work we show how such correlations can be modeled by two one-electron systems linked via a *constraint*.

In classical dynamics, constraints appear as some algebraic relations between generalized coordinates of a system and their time derivatives (velocities), which are to hold for any moment of time. They are widely used to model, e.g., effects of an environment on a system in question, or to develop theories with local symmetries (gauge theories) such as electrodynamics, general relativity and Yang-Mills theories. Classical constrained dynamics has been well studied in classical works by d’Alambert, Lagrange, Hölder and Gauss (see, e.g., Ref. [18] and references therein). In quantum mechanics constraints have been analyzed by Dirac [19], mainly because of the need of quantizing fundamental physical theories with local symmetries. The question addressed by Dirac was the following: *Given a classical system with constraints, construct a quantum theory which satisfies the correspondence principle.* A time evolution of a quantum system is described by the evolution operator. Its kernel in the coordinate representation is called a quantum mechanical propagator. For constrained systems it is usually obtained by a reduction of the Feynman phase space path integral onto the physical phase space, as proposed by Faddeev [20]. There are many subtleties associated with quantization of constrained systems (see for a review, e.g., [21]).

Here we propose a quantum constrained system which can be used to model the charge transfer interaction between an F^- ion and a metal surface. The basic idea is to transform the original six-electron problem to two one-electron problems each of which describes a possible decay channel of the ion. As a consequence of the quantum equivalence of the outer-shell electrons, the effective one-electron systems turn out to be linked *only* by a constraint. In other words, the entire interaction between the two systems occurs through a constraint rather than via a local potential. One can also say that such a kinematic coupling of the decay channels is induced by the symmetry of the original six-electron problem.

The constraint has a remarkable feature: It does not have a classical limit, meaning that its effects disappear in the formal classical limit $\hbar \rightarrow 0$. That is, the dynamical effect modeled by such a constraint is essentially quantum and cannot be modeled by any classical

potential force. In this regard, the canonical quantization scheme for constrained systems due to Dirac is not applicable here. We develop below a novel computational scheme for a quantum evolution subject to such purely quantum constraints. The scheme is based on the projection formalism introduced earlier by one of us [22] within the framework of gauge theories. Our approach also comprises a novel method to account for the intra-atomic correlations within a one-electron description of the charge transfer interaction between an F^- ion and the $Cu(111)$ and $Ag(111)$ surfaces. We demonstrate that the approach turns out to be very efficient in the wave packet propagation studies.

The choice of the $F^-/Cu(111)$ and $F^-/Ag(111)$ systems is motivated by several reasons. The interaction of halogen negative ions with a free-electron metal surface has already been studied theoretically within the Coupled Angular Mode approach which lead to a quite satisfactory description of the halogen negative ion formation in scattering halogen atoms by various metal surfaces [12,13]. Recently, on the example of the $Cu(111)$ surface it has been shown that the projected band gap of the (111) surfaces of noble metals strongly affects the RCT [23,24]. The point is that in a certain energy range electrons cannot propagate along the normal to the surface (L-band gap in the $\langle 111 \rangle$ direction [25]). On the other hand, the RCT process corresponds to an electron tunneling between the atom and the surface which is favored along the surface normal. In addition, it was shown that the 2D electronic continuum of the surface state plays a significant role, often dominating the RCT process. The band gap has several consequences. First, there exist very long lived states in the alkali- $Cu(111)$ systems [24,26,27]. Second, there is a parallel velocity dependence of the probability of an electron capture by the atom from $Cu(111)$ surfaces in grazing scattering experiments that is characteristic of a 2D electronic continuum [28]. Third, there exists an avoided crossing between the energy level of the projectile and the bottom of the surface state continuum [23]. These effects have been found to depend strongly on the interaction time [23,29,30]: They only appear for long interaction times, i.e., for slow collisions.

The free F^- ion energy level is slightly above the bottom of the surface state continuum of the $Cu(111)$ and $Ag(111)$ surfaces, and therefore, because of the image charge attraction,

it could cross the bottom of the 2D continuum for a finite ion-surface distance. In the present work, we investigate the effects of the projected band gap and of the surface state continuum on the F^- -metal charge transfer. In particular, we study the behavior of the system when the ion energy level is very close to the bottom of the 2D surface state continuum. A Wave Packet Propagation (WPP) approach to the RCT [8,23] provides a quantitative description of dynamic and static aspects of the F^- -surface charge transfer. The latter allows one to analyze the dependence of the band structure effect upon an interaction time in the RCT.

II. METHOD

A. A negative ion F^-

The free negative ion F^- is usually described in the Hartree–Fock approximation as a closed shell ion with the electronic configuration $1s^2 2s^2 2p^6$. Its binding energy is 3.4 eV. In this approach the outer shell electrons are regarded as equivalent. Their wave function is given by the corresponding Slater determinant

$$\Phi = \frac{1}{\sqrt{6!}} \left| 2p_0^\alpha 2p_0^\beta 2p_1^\alpha 2p_1^\beta 2p_{-1}^\alpha 2p_{-1}^\beta \right| , \quad (1)$$

where $2p$ symbolizes a $2p$ orbital wave function, the superscripts α and β stand for the two possible spin directions, and the subscript indicates the magnetic quantum number m corresponding to the projection of the $2p$ angular momentum on the quantization axis. The Slater determinant (1) can be expanded into a sum of products of wave functions of an ionic core and an outer electron:

$$\Phi = \frac{1}{\sqrt{6}} \sum_{j=1}^6 |F_j| A_j \phi_j = \sum_{j=1}^6 |G_j| \phi_j , \quad (2)$$

where the five-electron determinant $|F_j|$ describes a state of the fluorine atom $F(^2P)$. The product $A_j \phi_j$ corresponds to the $2p_m^{\alpha,\beta}$ orbital, which has been factorised into a spin factor A_j and a spatial wave function $\phi_j = \phi_j(\vec{r})$. The wave function (2) can also be used for an open shell description of the negative ion of the type $2p^5 2p'$. In this case, the spatial

wave function ϕ_j singled out in (2) corresponds to the outer $2p'$ orbital of the negative ion, whereas the core wave function $|G_j|$ is formed by the inner $2p$ orbitals. When analyzing the electron detachment process in the open shell description, the $2p'$ orbital is regarded as an active one.

The representation (2) is particularly well suited for an analysis of the electron capture/loss process between a fluorine ion F^- and a metal surface since it gives an expansion of the ion wave function over possible detachment channels. So, we retain the representation (2) to describe a loss or capture of an electron by the fluorine core

$$\Psi = \sum_j |G_j| \psi_j . \quad (3)$$

Here $\psi_j = \psi_j(\vec{r})$ is a wave function of an electron (captured or lost) in the j -channel. Neglecting the spin-orbit interactions and assuming the ion-surface interaction to be invariant under translations of the ion parallel to the surface, the system becomes invariant under the spin flip and rotations about the z -axis which is set to be perpendicular to the metal surface and passing through the ion center. Next, the z -axis is chosen as the quantization axis. Therefore the states with the z -component of the electron angular momentum ± 1 are degenerate. As a consequence, only two electron wave functions are distinct in the representation (3). They correspond to the states with $m = 0$ and $|m| = 1$. In what follows we assume that the charge transfer does not affect the neutral core wave function $|G_j|$. Only the outer electron is subject to the RCT dynamics.

Any state of the system can be represented as a two dimensional isovector $|\Psi\rangle$ whose components are one-electron states corresponding to $m = 0$ and $|m| = 1$ (upper and lower elements of the isovector, respectively). In cylindrical coordinates (z, ρ, φ) , it can be written as

$$\langle \vec{r} | \Psi \rangle = \begin{pmatrix} \psi_0(z, \rho) \\ \psi_1(z, \rho) e^{i\varphi} \end{pmatrix} . \quad (4)$$

Note that, due to the symmetry of the problem, the φ dependence can be explicitly given. Hence, one can limit oneself to studying the z - and ρ -dependence of the electron wave packet.

In our representation a free ion wave function is given by

$$\langle \vec{r} | \Psi_{F^-} \rangle = \begin{pmatrix} \frac{1}{\sqrt{3}} p(r) Y_{10}(\theta, \varphi) \\ \sqrt{\frac{2}{3}} p(r) Y_{11}(\theta, \varphi) \end{pmatrix} \quad (5)$$

where $p(r)$ is the radial part of the free-ion orbital and $Y_{lm}(\theta, \varphi)$ are the spherical harmonics. The different normalization factors of the isovector components are due to the fact that the free ion wave function (2) contains twice as many states with $|m| = 1$ as with $m = 0$. The functions $p(r)Y_{lm}(\theta, \varphi)$ have a unit norm so that $\langle \Psi_{F^-} | \Psi_{F^-} \rangle = 1$.

Yet another remark is that the approach outlined above assumes that only an outer electron can be detached (the detachment occurs through the evolution of the wave functions ψ_0 and ψ_1), i.e., it assumes an open shell description ($2p^5 2p'$) of the ion F^- . A closed shell description ($2p^6$) would correspond to an increase of the charge transfer interaction by the factor $\sqrt{6}$, and, hence, to an increase of the width by the factor 6 (see a discussion in [16]). This appears to be better adapted for the halogen negative ion case.

With all the above settings, a modeling of the charge transfer in the F^- -metal system implies finding a one-electron Hamiltonian that governs a time evolution in the Hilbert space spanned by vectors (4). We take it in the following form

$$\mathbf{H} = \mathbf{T} + \mathbf{V}_{\text{at}} + \mathbf{V}_{\text{S}} = \mathbf{H}_{\text{at}} + \mathbf{V}_{\text{S}} . \quad (6)$$

The operators \mathbf{H} , \mathbf{T} , \mathbf{V}_{at} , \mathbf{V}_{S} and \mathbf{H}_{at} are diagonal 2×2 matrices, in fact, we choose them to be proportional to a unit 2×2 matrix, with the diagonal elements denoted, respectively, H , T , V_{at} , V_{S} and H_{at} . Here, T is the electron kinetic energy operator, V_{at} the potential of the interaction between an electron and the neutral core, V_{S} the potential of the electron-surface interaction, $H_{\text{at}} = T + V_{\text{at}}$, and $H = H_{\text{at}} + V_{\text{S}}$. The wave functions $p(r)Y_{lm}(\theta, \varphi)$ are eigenfunctions of the one-electron Hamiltonian H_{at} .

The time evolution of the wave function (4) generated by the Hamiltonian (6) is nothing but the evolution of two independent one-electron wave packets. On the other hand, the two components of the isovector (4) cannot evolve independently. Indeed, in the free ion case, the two components cannot be arbitrarily chosen in order for the state (4) to describe a physical

free ion. Actually, the radial components of the column elements appear to be proportional to each other with a specific factor (cf. (5)). This relation between the two components comes from the expansion of the Slater determinant (1) which possesses a high symmetry being the symmetry of a quantum system of identical particles occupying the same energy level. The very same symmetry must be preserved in the expansion (2) and, hence, upon a reduction of the six-electron description to our one-electron formalism. In other words, there must be a correlation between evolving components of the isovector corresponding to the electron states with $m = 0$ and $|m| = 1$ thanks to the symmetry of the six-electron problem. Therefore physically admissible states in the Hilbert space spanned by isovectors (4) must be subject to some constraints required by the symmetry of the original six-electron problem. This will be a key point of our new approach to the RCT dynamics.

To illustrate the necessity of constraints, consider the case when the detachment occurs in the $m = 0$ channel. Then the bound part of the $|m| = 1$ channel must also disappear at the same time because there is only one ion F^- which contains both $m = 0$ and $|m| = 1$ components. In the Effective Range approach [31] used in the Coupled Angular Mode (CAM) method [6], this problem has been solved in the following way. One only considers the wave function of the system given by expression (4) outside a spherical region of radius r_c . The F core is contained in the region. The boundary condition on the radial components ψ_0 and ψ_1 at $r = r_c$ couples the two channels. This approach essentially relies on the use of spherical coordinates. Here we look for a coordinate independent description of the channel mixing that can be *efficiently implemented in numerical calculations of the time evolution of the system (wave packet propagation)*. The origin of the kinematic coupling of the channels is now sought in symmetries of the system. It is believed that such an approach is rather general and could be applied to other many-electron systems where a conventional mean field approach does not provide a good approximation.

The basic idea is that the Hilbert space spanned by isovectors (4) is too large and contains states which are physically not acceptable. It is clearly seen already from the fact that the radial components of the free ion state (5) are not independent. We shall then constrain the

state (4) to allow only one bound ion F^- of the form (5). Any other state with components $\psi_0 \sim p(r)Y_{10}(\theta, \varphi)$ and $\psi_1 \sim p(r)Y_{11}(\theta, \varphi)$ should be forbidden. This corresponds to making the state (4) orthogonal to the vector

$$\langle \vec{r} | Q \rangle = \begin{pmatrix} \sqrt{\frac{2}{3}} p(r) Y_{10}(\theta, \varphi) \\ -\sqrt{\frac{1}{3}} p(r) Y_{11}(\theta, \varphi) \end{pmatrix} \equiv \begin{pmatrix} p_0(z, \rho) \\ -p_1(z, \rho) e^{i\varphi} \end{pmatrix}. \quad (7)$$

Since the state (7) cannot also occur as a virtual (or intermediate) state of the ion in the time evolution of the system, we demand that the time dependent wave packet (4) must be orthogonal to the vector $|Q\rangle$:

$$\langle Q | \Psi(t) \rangle = \langle p_0 | \psi_0(t) \rangle - \langle p_1 | \psi_1(t) \rangle = 0, \quad (8)$$

for any $t \geq 0$, where $\langle p_{0,1} | \psi_{0,1}(t) \rangle$ stands for a standard scalar product (written in cylindrical coordinates because the functions $p_{0,1}$ and $\psi_{0,1}$ depend on z and ρ only).

From the physical point of view the constraint (8) simply means that there is an unwanted scattering mode in our effective one-electron problem. Although the Hamiltonian may allow for such a mode, we have given physical reasons to forbid it. The constraint (8) implies that the time evolution of the two components of the isovector (4) is no longer independent even though the Hamiltonian (6) does not provide any direct coupling of them. The link between the detachment channels with $m = 0$ and $|m| = 1$ steams directly from the free ion structure. It implicitly assumes that the correlation between the wave functions ψ_0 and ψ_1 in the ion perturbed by an interaction with a metal surface is the same as in the free ion. Thus, the electronic structure of F^- has been modeled by two one-electron problems linked by the constraint (8).

B. Physical Hamiltonian

Now we face a problem of incorporating the constraint into quantum dynamics generated by the Hamiltonian (6). The difficulty is clear. Suppose an initial state satisfies the constraint (8). Applying the evolution operator $\exp(-it\mathbf{H})$ to it, we immediately observe

that the evolved state fails to satisfy the constraint. The procedure we propose is based on the projection operator formalism first introduced for gauge theories [22,32]. It has been generalized to general constrained systems [33,34] (see also the review [21]). The key steps are as follows.

Consider the projection operator

$$\mathbf{P} = \mathbf{I} - |Q\rangle \langle Q|, \quad (9)$$

where \mathbf{I} is the unit operator, $\mathbf{I} |\Psi\rangle = |\Psi\rangle$ for any $|\Psi\rangle$. It is easy to convince oneself that the operator (9) is self-adjoint, $\mathbf{P}^\dagger = \mathbf{P}$, and satisfies the characteristic property of a projection operator, $\mathbf{P}^2 = \mathbf{P}$. By construction, the state $\mathbf{P} |\Psi\rangle$ satisfies the constraint (8) for any state $|\Psi\rangle$. The operator (9) projects any state to the physical subspace defined by the condition (8). In particular, $\mathbf{P} |Q\rangle = 0$. To eliminate the state $|Q\rangle$ as a possible intermediate state of the system in the time evolution, the Hamiltonian is projected onto the physical subspace

$$\mathbf{H} \rightarrow \mathbf{PHP} = \mathbf{H}_{\text{phys}}. \quad (10)$$

The physical Hamiltonian (10) is self-adjoint. Hence the time evolution generated by it is unitary. The state $\mathbf{PHP} |\Psi\rangle$ satisfies the constraint (8). Clearly, the physical Hamiltonian is nonlocal, in general, even if the original Hamiltonian has a standard form of the sum of potential and kinetic energies. However, classical limits of \mathbf{H} and \mathbf{H}_{phys} are the same.

The evolution operator has the form

$$\mathbf{U}(t_1, t_2) = \mathbf{P} \text{T exp} \left(-i \int_{t_1}^{t_2} d\tau \mathbf{PHP} \right) \mathbf{P} = \mathbf{P} \exp(-it\mathbf{PHP}) \mathbf{P}, \quad (11)$$

where $t = t_2 - t_1$ and T exp stands for the time ordered exponential. The second equality holds when the Hamiltonian \mathbf{H} does not explicitly depend on time. The projection operators before and after the exponential in (11) can be omitted if the initial state satisfies the constraint (8).

The physical Hamiltonian provides the sought-for channel mixing. To find terms in the new Hamiltonian which give rise to the channel mixing, we compute the action of \mathbf{PHP} on a generic state $|\Psi\rangle$. A straightforward computation leads to the following result

$$\begin{aligned}
\mathbf{PHP} |\Psi\rangle &= \begin{pmatrix} H |\psi_0\rangle - \lambda_1(H + \lambda_2) |p_0\rangle - \lambda_2 |p_0\rangle \\ H |\psi_1\rangle - \lambda_1(H + \lambda_2) |p_1\rangle - \lambda_2 |p_1\rangle \end{pmatrix}, \\
\lambda_1 &= \langle Q|\Psi\rangle = \langle p_0|\psi_1\rangle + \langle p_1|\psi_2\rangle, \\
\lambda_2 &= \langle Q|\mathbf{V}_S|\Psi\rangle = \langle p_0|V_S|\psi_0\rangle + \langle p_1|V_S|\psi_1\rangle.
\end{aligned} \tag{12}$$

If the state $|\Psi\rangle$ belongs to the physical subspace then, according to (8), $\lambda_1 = 0$. However, the action of \mathbf{PHP} even on the physical states is not reduced to that of \mathbf{H} because the amplitude λ_2 is generally not zero. Thus, after the projection (10) the original Hamiltonian (6) acquires an additional term

$$\mathbf{PHP} = (\mathbf{H} + \mathbf{W}) P \tag{13}$$

$$\mathbf{W} = -|Q\rangle \langle Q| V_S. \tag{14}$$

The operator \mathbf{W} provides the channel mixing even if the initial state is in the physical subspace. The correlation between the two components of $|\Psi\rangle$ is a consequence of the unbalanced action of the operator V_S on the components of $|\Psi\rangle$. It vanishes in the limit of the free negative ion.

C. Interaction potentials

The potential V_{at} in the Hamiltonian (6) represents the interaction between the active electron and the fluorine neutral core. It is taken as a local model potential which depends on the distance r between the electron and the atom center. The potential also includes a long range polarization interaction. Its explicit form has been adjusted to reproduce the binding energy of the ion F^- as well as the mean radius of the p -orbital. The potential reads

$$\begin{aligned}
V_{\text{at}} &= -U_0 + gr^2 - ae^{-r^2}, & r \leq 1; \\
V_{\text{at}} &= -\frac{\alpha}{2r^4} - ae^{-r^2}, & r > 1,
\end{aligned} \tag{15}$$

where $U_0 = 5.64$, $g = 3.76$, $a = 1.2558$ and the atomic polarizability of a fluorine atom $\alpha = 3.76$ [35]. All constants are given in the atomic units.

The potential V_S in the Hamiltonian (6) describes the interaction of the active electron with the $Cu(111)$ and $Ag(111)$ surfaces. It has been proposed by Chulkov et al on the basis of their *ab initio* studies [36]. This local potential depends only on the electron coordinate z along the surface normal. Its explicit form can be found in Ref. [36]. Qualitatively, it is an image charge potential in vacuum which joins smoothly an oscillating potential with the period being that of the (111) planes inside the metal bulk. When describing an electron motion in the direction perpendicular to the $Cu(111)$ or $Ag(111)$ surface, this potential represents rather well important features of the surface such as the projected band gap (between -5.83 and -0.69 eV with respect to vacuum for Cu and between -4.96 and -0.66 eV for Ag), the surface state (5.33 eV and 4.625 eV below vacuum for $Cu(111)$ and $Ag(111)$, respectively), and the image state energy positions (0.82 eV and 0.77 eV below vacuum, respectively, for $Cu(111)$ and $Ag(111)$). Since the RCT process mainly favors transitions around the surface normal, this potential is expected to account for the effect of the peculiarities of the $Cu(111)$ and $Ag(111)$ surfaces.

In order to illustrate the effects of the projected band gap of the $Cu(111)$ and $Ag(111)$ surfaces, we also present results obtained for a free-electron description of the metal surface. In this case, the local electron-surface interaction potential corresponds to the $Al(111)$ surface and is taken from the work of Jennings et al [37].

D. Wave packet propagation

In the wave packet propagation (WPP) approach [8,23], one studies the time evolution of an electron wave function $\langle \vec{r} | \Psi(t) \rangle$ generated by the system Hamiltonian. Here we consider both the static and dynamic problems. In the former, the distance between the ion and the metal surface is fixed, while in the latter the ion collides with the surface. In both cases, the initial state is the free ion state (5).

The time evolution can be regarded as a sequence of infinitesimal time steps generated by the evolution operator (11)

$$|\Psi(t + \Delta t)\rangle = \mathbf{U}(t, t + \Delta t) |\Psi(t)\rangle. \quad (16)$$

Since the initial state $|\Psi(t = 0)\rangle = |\Psi_{F-}\rangle$ is orthogonal to the vector $|Q\rangle$, i.e., it is in the physical subspace, we can omit the projection operators to the left and right of the exponential in (11). So in (11) we take

$$\mathbf{U}(t, t + \Delta t) = e^{-i\Delta\mathbf{P}\mathbf{H}\mathbf{P}} = e^{-i\Delta t(\mathbf{H}_{\text{at}} - E_a|Q\rangle\langle Q| + \mathbf{P}\mathbf{V}_S\mathbf{P})}, \quad (17)$$

where the property $\mathbf{H}_{\text{at}}|Q\rangle = E_a|Q\rangle$ of the vector $|Q\rangle$ has been used; E_a is the eigenvalue of H_{at} corresponding to the eigenfunctions $p(r)Y_{l,m}(\theta, \varphi)$ with $l = 1$ and $m = 0, \pm 1$. For an infinitesimal time step Δt , the action of the evolution operator (17) can be evaluated by means of the split operator approximation [38,39]

$$\mathbf{U}(t, t + \Delta t) = e^{-i\frac{\Delta t}{2}\mathbf{P}\mathbf{V}_S\mathbf{P}} e^{-i\Delta t(\mathbf{H}_{\text{at}} - E_a|Q\rangle\langle Q|)} e^{-i\frac{\Delta t}{2}\mathbf{P}\mathbf{V}_S\mathbf{P}} + O(\Delta t^3). \quad (18)$$

Making use of the commutation relation of \mathbf{H}_a and $|Q\rangle\langle Q|$, this representation can be further simplified

$$\mathbf{U}(t, t + \Delta t) = e^{-i\frac{\Delta t}{2}\mathbf{P}\mathbf{V}_S\mathbf{P}} \left\{ \left(e^{i\Delta t E_a} - 1 \right) |Q\rangle\langle Q| + \mathbf{I} \right\} e^{-i\Delta t \mathbf{H}_{\text{at}}} e^{-i\frac{\Delta t}{2}\mathbf{P}\mathbf{V}_S\mathbf{P}} + O(\Delta t^3). \quad (19)$$

The action of the exponential involving V_S is evaluated via a Taylor expansion in which four terms are typically kept for the time step $\Delta t = 0.025$ atomic units.

The action of the kinetic energy operator is computed in the cylindrical coordinates which are well suited to the symmetry of the problem

$$T = -\frac{1}{2} \frac{\partial^2}{\partial z^2} - \frac{1}{2\rho} \frac{\partial}{\partial \rho} \rho \frac{\partial}{\partial \rho} + \frac{m^2}{2\rho^2} \equiv T_z + T_\rho, \quad (20)$$

where T_z contains only the z -derivative. The exponential of \mathbf{H}_{at} in (19) is then transformed as

$$e^{-i\Delta t \mathbf{H}_{\text{at}}} = e^{-i\Delta t H_{\text{at}}} \mathbf{I} = e^{-i\frac{\Delta t}{2}(T_z + V_{\text{at}})} e^{-i\Delta t T_\rho} e^{-i\frac{\Delta t}{2}(T_z + V_{\text{at}})} \mathbf{I} + O(\Delta t^3). \quad (21)$$

Recall that the operator \mathbf{H}_{at} is diagonal in the isotopic two-dimensional space. So, the operator (21) acts on both components of $|\Psi(t)\rangle$ in the same way. Finally, all the exponentials in (21) are approximated by means of the Cayley representation [40]

$$e^{-i\Delta t A} = \frac{1 - i\frac{\Delta t}{2} A}{1 + i\frac{\Delta t}{2} A} + O(\Delta t^3) . \quad (22)$$

In order to accurately reproduce the wave packet variation close to the atom center, we use a mapping procedure [41,42] defined by

$$\begin{aligned} z = f(\xi) &= 0.05\xi + \frac{0.95\xi^3}{400 + \xi^2} , \\ \rho = f(\eta) &= 0.05\eta + \frac{0.95\eta^3}{400 + \eta^2} , \\ \langle z, \rho | \Psi(t) \rangle &= \frac{1}{\sqrt{\rho}} \tilde{\Psi}(t, z, \rho) . \end{aligned} \quad (23)$$

The wave packet $\tilde{\Psi}(t, z, \rho)$ is evaluated on a 2D mesh of points (ξ_k, η_j) of the size 1200×800 with the step size $\Delta = 0.2$ atomic units for both the coordinates. At the grid boundary, an absorbing potential is introduced [43,44] in order to avoid the wave packet reflection.

The kinetic energy operator (20) has to be written in the auxiliary variables ξ and η and then discretized. After the change of variables (23) the operator T_ρ assumes the form

$$T_\rho = -\frac{1}{2} \frac{1}{J\sqrt{f}} \frac{\partial}{\partial \eta} \frac{f}{J} \frac{\partial}{\partial \eta} \frac{1}{\sqrt{f}} + \frac{1}{2} \frac{m^2}{f^2} , \quad (24)$$

where $J(\eta) = f'(\eta)$ is the Jacobian. The grid in the η -coordinate is set as $\eta_j = \Delta/2 + \Delta(j-1)$. For every value ξ we have $\tilde{\Psi}_j = \Psi(\xi, \eta_j)$, and the action of (24) is defined by the following midpoint procedure

$$(T_\rho \tilde{\Psi})_j = -\frac{1}{2\Delta^2} \frac{1}{J_j \sqrt{f_j}} \left[\frac{f_{j+1/2}}{J_{j+1/2}} \left(\frac{\tilde{\Psi}_{j+1}}{\sqrt{f_{j+1}}} - \frac{\tilde{\Psi}_j}{\sqrt{f_j}} \right) - \frac{f_{j-1/2}}{J_{j-1/2}} \left(\frac{\tilde{\Psi}_j}{\sqrt{f_j}} - \frac{\tilde{\Psi}_{j-1}}{\sqrt{f_{j-1}}} \right) \right] + \frac{1}{2} \frac{m^2}{f_j^2} . \quad (25)$$

Here the subscript $j \pm 1/2$ means that the corresponding function is taken at the midpoint $\eta_j \pm \Delta/2$. A similar expression can be obtained for the action of T_z on the grid $\xi_k = \xi_0 + \Delta(k-1)$.

In the first series of calculations, we study the static problem when the ion F^- is at a fixed distance Z from the metal surface. The survival amplitude of the ion (the auto-correlation of the wave function) is given by

$$A(t) = \langle \Psi(t=0) | \Psi(t) \rangle . \quad (26)$$

From the Laplace transform of the function $A(t)$, one can obtain the density of states (DOS) projected on the free ion wave function. The structure of the DOS yields the energy level and its width for the negative ion state interaction with the surface. In what follows, this width is referred to as the “static width” to emphasize that it is extracted from static calculations. It gives the electron transfer rate between the negative ion and the metal surface in the static problem.

In the second series of calculations, we study the evolution of the electron wave packet when a negative fluorine ion collides with the surface. The ion is assumed to approach the surface along a straight line perpendicular to the surface at a constant velocity v . Only the incoming part of the collision is studied. The time dependence of the wave function is obtained in the projectile reference frame, i.e., the time dependence of the Hamiltonian occurs through the potential V_S . For each collision velocity, the ion survival probability, $P(t, v) = |A(t, v)|^2$, is computed. To analyze the dynamics of the charge transfer, we define an effective width of the negative ion state by

$$G(Z, v) = -\frac{\partial \log[P(t, v)]}{\partial t} , \quad (27)$$

where $Z = Z_0 - vt$ with Z_0 being an initial distance of the ion from the metal surface. It corresponds to an effective decay rate of the ion when it approaches the surface with a velocity v . Comparing $G(Z, v)$ to the level width obtained in the static calculations allows us to see to what extent the dynamical evolution can be described by the static width of the ion level.

III. RESULTS AND DISCUSSION

A. F^- ions interacting with a surface $Al(111)$

The interaction of an F^- ion with an $Al(111)$ surface, where the latter is regarded as a free-electron metal surface, has already been studied by the CAM method associated with the effective range treatment of the negative ion [12,13]. It lead to a successful description of the negative ion formation in a grazing angle scattering [12]. Similarly, for large angle scattering from $Ag(110)$, and polycrystalline Ag and Al surfaces, a quantitative agreement with experiment results [14,45] has been obtained [13].

In Figures 1 and 2 we compare the results obtained in the static case by two different methods: The CAM method with effective range treatment of the negative ion and the present WPP results obtained with the projection formalism. In both cases, the $Al(111)$ surface is described as a free-electron metal surface using the potential proposed in [37]. Figures 1 and 2 present, respectively, the energy position and the width of the F^- ion level interacting with the surface as a function of the ion-surface distance Z measured from the image plane. The characteristics of the ion level as a function of Z display the behavior common for atomic species in front of a free-electron surface: The energy of the negative ion state decreases as the ion is placed closer to the surface, which can be anticipated because of the image charge attraction; The level width increases roughly exponentially as Z decreases. The results obtained by two different methods are extremely close to each other. This gives confidence in the equivalence of the two descriptions of the F^- ion. The results for a free-electron $Al(111)$ surface are used below as a “free electron” reference to which compare the $Cu(111)$ and $Ag(111)$ results. It appears that the free electron results are almost identical for the three metals, except at very small distances from the surface.

B. F^- ions interacting with a surface Cu(111). A static case

Figures 3 and 4 present the F^- ion level characteristics (energy (Fig.3) and width (Fig.4)) as a function of the ion-Cu(111) surface distance. The negative ion level energy exhibits an avoided crossing around $4a_0$ from the surface, which is quite different from the smooth behaviour seen in Figures 1 and 2 for the free-electron metal. This is a direct consequence of the peculiarities of the Cu(111) surface and a similar situation has already been observed in the case of H- interacting with the same surface [23].

A schematic picture of the electronic structure of the model Cu(111) surface is shown in Fig. 5. The energy of electronic levels is plotted as a function of the electron momentum, k_{\parallel} , parallel to the surface. For k_{\parallel} equal to zero, the projected band gap lies within the energy range from -5.83 to -0.69 eV (with respect to vacuum). Inside the gap, there is a surface state at -5.33 eV. In the present model of a Cu surface, the dispersion curves of all the metal electronic states as functions of k_{\parallel} are parabolic with a free-electron mass.

The resonant charge transfer process corresponds to transitions between the ion level and metal states of the same energy. At large distances, the F^- ion level is degenerate with the band gap. Therefore it can only decay to metal states with a finite k_{\parallel} i.e. either to the 2D surface state band, or into 3D propagating states. As Z decreases, the energy of the negative ion state decreases and it comes close to the bottom of the 2D surface state continuum. The ion can decay by ejecting an electron with the angular momentum $m = 0, \pm 1$ (the quantization axis is normal to the surface). As explained in Ref. [23], a resonance cannot cross the bottom of a 2D continuum in the symmetrical case $m = 0$ and there always exists a bound state below the bottom of the continuum. This state has an avoided crossing with the state which becomes the free ion state as Z tends to infinity. The F^- ion character is then found to be associated with two different states depending on the Z range. It is transferred from the upper to the lower state when going through the crossing region (decreasing Z). Far from the avoided crossing region, the ion energy level is rather close to that found in the free electron case.

As for the width, at large Z , its absolute value for F^- in front of the $Cu(111)$ surface is larger than that in the case of a free-electron surface. This result might appear surprising since the projected band gap prohibits the electron transfer from the projectile to the metal along the surface normal ($k_{\parallel} = 0$) and blocks the RCT into the 3D bulk continuum. Indeed, as can be seen in Fig. 5, there are no electronic states of the metal with small k_{\parallel} which are in resonance with the negative ion state. The potential barrier separating the ion and the surface attains its least value in the direction normal to the surface. Therefore, the surface normal is the preferred direction of the resonant electron transfer. One would then expect that the effect of the projected band gap would be to stabilize the negative ion level as compared with the case of a free electron metal. This has indeed been found for H^- interacting with $Cu(111)$ where the width of the H^- state was much reduced as compared to the $H^-/Al(111)$ - case [23].

In contrast, we have observed an increase of the fluorine negative ion decay rate as compared to the free-electron metal case. The reason is twofold. First, the 2D surface state continuum contributes to the decay of F^- . Second, a fluorine has a much larger electron affinity than a hydrogen. Thanks to a better overlap of the wave functions, the 2D surface state continuum, when energetically allowed, is a dominating decay channel for an ion state lying within the band gap [23,28,46]. Moreover, when the binding energy of a negative ion is close to that of the surface state, a coupling of the ion level with the 2D surface state continuum is more efficient than its coupling with the 3D continuum of the free-electron metal states (see a discussion in [46]). The efficiency of the 2D surface state continuum as a decay channel can also be deduced from the sharp decrease of the level width when passing through the crossing region as Z decreases, i.e., when this decay channel becomes closed.

For small values of Z : (i) the 2D surface state continuum does not contribute to the decay of the negative ion, and (ii) the energy of the negative ion state is very close to the bottom of the projected band gap for small k_{\parallel} so that the band structure effect for the decay into the 3D bulk continuum vanishes. Therefore, we find the width of the level with ionic character very close to the free-electron results.

Finally, we can stress that the procedure of extracting the resonance characteristics employed here is based on the autocorrelation function (26) using the free F^- ion wave function as the initial state. It converges well for the states of an ionic type. Convergence of the resonance characteristics for other states is difficult to achieve. This is the reason for showing only one state far from the crossing region (small or large Z). In the crossing region, the ionic character is shared between the lower and upper states so that the characteristics (energy and width) of both of them can be extracted. Since the convergence is easier to achieve for the energy of the state, the interval of distances Z where both states are presented is larger in Fig.3.

C. F^- ions interacting with an $Ag(111)$ surface. Static and dynamic studies

The electronic structures of $Ag(111)$ and $Cu(111)$ look rather similar (cf. Figures 5 and 6). However, characteristic features of the electronic structures occur at different energies. The surface state in $Ag(111)$ is located higher in energy than in $Cu(111)$. For this reason the avoided crossing appears at a larger Z where the ion-surface charge transfer interaction is smaller. As a consequence the avoided crossing could not be resolved in the energy dependence because it is localised in a too small range of Z . Therefore, we have chosen to represent the results for the energy and the width by a single continuous line (Figures 7 and 8, respectively). In fact, the energy of the negative ion state is almost the same as for the free-electron metal surface. The characteristic change of the level width when passing the crossing region (decreasing Z) is however still perfectly visible. It fully confirms the dominance of the 2D surface state channel in the F^- ion decay at large Z .

At small Z , the F^- ion level is embedded in the 3D propagating states of Ag and its characteristics are very close to those of the free-electron case. Very close to the surface, the decrease of the level width as compared to $Al(111)$ free-electron results is caused by the closeness of the F^- level to the bottom of the $Ag(111)$ valence band. As can be seen in Fig. 3b the bottom of the $Ag(111)$ valence band is located at -9.7 eV in our model description

of the $Ag(111)$ surface. For the model free-electron $Al(111)$ case it is located at -15.9 eV.

By studying the time dependent problem, one can find out whether the peculiarities of $Ag(111)$ observed in the static case can still be visible in a collision of F^- with the $Ag(111)$ surface. We have computed the effective level width G , defined by (27), as a function of the distance for an ion F^- approaching the surface at different velocities. The results are displayed in Fig. 9 together with the results of the static case for $Ag(111)$ and the free-electron metal surface $Al(111)$. As the collision velocity is increased, the effective width becomes closer to the free-electron result. This feature is very similar to what we have found for ions H^- interacting with a $Cu(111)$ surface [23]. The system needs a finite time to react on the presence of the projected band gap. If the collision is too fast, the electron wave packet does not have enough time to “explore” the band structure of the metal, and the ion decay remains identical to that on a free-electron metal surface.

In contrast, as the collision velocity is decreased, the effective width comes nearer to the static $Ag(111)$ width. For the smallest velocity used here, 0.0058 atomic units which correspond to a collision energy about 16 eV, the effective width is very close to the static one at large Z . When Z is decreased, the effective width fails to perfectly reproduce the change of the behavior associated with the crossing of the bottom of the surface state continuum for all collision velocities considered here. We can nevertheless see that this variation is better reproduced as the collision velocity is decreased. In fact, the dynamical broadening introduced by the change of the negative ion state energy with time [47] makes it impossible to reproduce a sharp variation of the static width as the ion approaches the surface. This leads to rounded delayed structures displayed in Fig.9. Moreover, the oscillations of the effective width at small Z can tentatively be attributed to the population transfer between the two adiabatic states at the crossing region. From these results one can conclude that in the studied collision energy range, 16 eV – 5 keV, the charge transfer rate is intermediate between the free-electron case and the static $Ag(111)$ case.

The formation of F^- ions and H^- ions by collision on a $Ag(111)$ surface has been studied experimentally by Guillemot and Esaulov [29]. When comparing with results obtained with

free-electron like surfaces they found that the H^- data presents a strong band gap effect. In particular, the survival probability of the negative ions leaving the surface was much larger for $Ag(111)$. This was attributed to the blocking of the resonant charge transfer in $H^-/Ag(111)$ system, in line with theoretical results obtained for $H^-/Cu(111)$ [23] where the RCT rates are reduced by orders of magnitude compared to the free-electron case. At the same time, results obtained with F^- ions were approximately consistent with a description based on the charge transfer rate obtained in the framework of a free-electron description of the metal surface. In the energy range studied in their work, as shown above, the dynamical behaviour of the charge transfer is intermediate between the free-electron and static $Ag(111)$ limits. This prohibits the use of the simple classical treatment of the parallel velocity effect [28,48] which was shown to be important for a formation of F^- , even at rather low collision energy [13]. Consequently, we cannot quantitatively compare our results with theirs. Nevertheless, we can notice that in our study the band gap effect is *reversed* and much smaller in the present system than in the $H^-/Cu(111)$ system; it is even partly suppressed by the ion motion. These findings qualitatively agree with the experimental results [29].

IV. CONCLUSIONS

We have reported on a study of the electron transfer in the ion-metal systems $F^-/Cu(111)$ and $F^-/Ag(111)$. We have developed a new method to describe the effect of six quasi-equivalent outer-shell electrons of F^- on the resonant charge transfer process. The original six-electron problem has been transformed into two one-electron problems in which the dynamics are not independent but rather are linked via a constraint. The projection formalism for quantum systems with constraints has been used to obtain the quantum mechanical propagator for such a system. This modeling of the ion F^- is simple, efficient and can easily be implemented in the wave packet propagation approach.

Both the $Cu(111)$ and $Ag(111)$ surfaces exhibit an electronic structure with a projected band gap in which the ion energy level lies at large ion-surface distances. This peculiarity

of the electronic structure influences the charge transfer interaction with the ion, leading to a few remarkable features:

- The ion level presents an avoided crossing with the bottom of the surface state continuum as predicted for a 2D continuum with $m = 0$. The avoided crossing is very clearly marked for the system $F^-/Cu(111)$.

- Because of the correlation between the six electrons of the F^- ion the avoided crossing, which is a characteristic feature of the symmetric case $m = 0$, appears in the present system where electrons in both states with $m = 0$ and $|m| = 1$ contribute to the charge transfer.

- When the negative ion level is low in the projected band gap, the band gap does not cause a drastic drop of the charge transfer rate as observed in other systems [23,24]. This feature of the charge transfer has been attributed to the following effects: (*i*) The band gap effect is expected to decrease as the projectile level is lower in the band gap; (*ii*) The decay to the surface state is favored over the decay to 3D bulk states because of a greater spatial overlap of the electron wave function with the surface state; and (*iii*) The polarization of negative ions does not enhance the band gap stabilization effect as it does for neutral atoms (see a discussion in Ref. [46]).

- At small ion-surface distances, when the negative ion state is not in the band gap or inside the gap but close to its bottom, the energy and the width of the negative ion level are practically identical to those found in the free-electron surface case.

- Studies of the corresponding dynamical systems, when the ion F^- approaches the surface, have shown that the above features survive, although partially, over a large collision energy range.

REFERENCES

- [1] J.A. Misewich, T.F. Heinz and D.M. Newns, Phys. Rev. Lett. 68 (1992) 3737
- [2] J.A. Prybyla, H.W.K. Tom and G.D. Aumiller, Phys. Rev. Lett. 68 (1992) 503
- [3] L. Bartels et al., Phys. Rev. Lett. 80 (1998) 2004
- [4] R. Hemmen and H. Conrad, Phys. Rev. Lett. 67 (1991) 1314
- [5] P. Nordlander and J.C. Tully, Phys. Rev. B 42 (1990) 5564
- [6] D. Teillet-Billy and J.P. Gauyacq, Surf. Sci. 239 (1990) 343
- [7] F. Martin and M.F. Politis, Surf. Sci. 356 (1996) 247
- [8] V.A. Ermoshin and A.K. Kazansky, Phys. Lett. A 218 (1996) 99
- [9] J. Merino, N. Lorente, P. Pou and F. Flores, Phys. Rev. B 54 (1996) 10959
- [10] S.A. Deutscher, X. Wang and J. Burgdörfer, Phys. Rev. A 55 (1997) 466
- [11] P. Kürpick, U. Thumm and U. Wille, Phys. Rev. A 56 (1997) 543
- [12] A.G. Borisov, D. Teillet-Billy, J.P. Gauyacq, J.A.M.C. Silva, A. Martens, C. Auth and H. Winter, Phys. Rev. B 59 (1999) 8218
- [13] N. Lorente, A.G. Borisov, D. Teillet-Billy and J.P. Gauyacq, Surf. Sci. 429 (1999) 46
- [14] S. Ustaze, L. Guillemont, V.A. Esaulov, P. Nordlander and D.C. Langreth, Surf. Sci. 415 (1998) L1027
- [15] R. Zimny, H. Nienhaus and H. Winter, Radiation Effects and Defects in Solids, 109 (1989) 9.
- [16] J.P. Gauyacq, A.G. Borisov and H. Winter, Comments in Modern Physics, Sect. D Atom. and Mol. Phys. 2 (2000) 29
- [17] H. Shao, D.C. Langreth and P. Nordlander, in: Low energy ion-surface interactions, Ed.

- by J.W. Rabalais (Wiley, New York, 1994) p. 118
- [18] V.I. Arnold, V.V. Kozlov and A.I. Neishtadt, Mathematical aspects of classical and celestial mechanics, in: Encyclopaedia of Mathematical Science, Vol. III, Dynamical Systems (Springer-Verlag, Berlin, 1988)
- [19] P.A.M. Dirac, Lectures on Quantum Mechanics (Yeshiva Univ., New York, 1964)
- [20] L.D. Faddeev, Theor. Math. Phys. 1 (1970) 1.
- [21] S.V. Shabanov, Phys. Reports 326 (2000) 1
- [22] S.V. Shabanov, in: Proceeding of "Path Integrals'96", Eds. V.S. Yarunin and M.A. Smondyrev, (JINR, Dubna, 1996) p. 133; LANL electronic archive, quant-ph/9608018; "Path Integral in Holomorphic Representation without Gauge Fixation", JINR preprint E2-89-678 (Dubna, 1989) (unpublished).
- [23] A.G. Borisov, A.K. Kazansky and J.P. Gauyacq, Phys. Rev. Lett. 80 (1998) 1996; Phys. Rev. B59 (1999) 10935
- [24] A.G. Borisov, A.K. Kazansky and J.P. Gauyacq, Surf. Sci. 430 (1999) 165
- [25] M.C. Desjonquères and D. Spanjaard, Concepts in Surface Science, Springer-Verlag Series in Surface Science, Vol. 40 (Springer-Verlag, Berlin, 1993)
- [26] M. Bauer, S. Pawlik and M. Aeschlimann, Phys. Rev. B 55 (1997) 10040
- [27] S. Ogawa, H. Nagano and H. Petek, Phys. Rev. Lett. 82 (1999) 1931
- [28] T. Hecht, H. Winter, A.G. Borisov, J.P. Gauyacq and A.K. Kazansky, Phys. Rev. Lett. 84 (2000) 2517
- [29] L. Guillemot and V.A. Esaulov, Phys. Rev. Lett. 82 (1999) 4552
- [30] L. Guillemot, S. Lacombe and V.A. Esaulov, Nucl. Inst. Meth. B 164-165 (2000) 601
- [31] D. Teillet-Billy, L. Malegat and J.P. Gauyacq, J. Phys. B 20 (1987) 3201

- [32] S.V. Shabanov, J. Phys. A24 (1991) 1199; and Phase Space Structure in Gauge Theories, JINR series of lectures, Vol. 54 (JINR, Dubna, 1989), P2-89-553
- [33] J.R. Klauder, Ann. Phys. (NY) 254 (1997) 419; Nucl. Phys. B547 (1999) 397
- [34] J.R. Klauder and S.V. Shabanov, Phys. Lett. B 398 (1997) 116; Nucl. Phys. B511 (1998) 713; Phys.Lett. B435 (1998) 343
- [35] Handbook of Chemistry and Physics, 5th Edition (CRC, Boca Raton, Florida, 1996)
- [36] E.V. Chulkov, V.M. Silkin and P.M. Echenique, Surf. Sci. 437 (1999) 330
- [37] P.J. Jennings, P.O. Jones and M. Weinert, Phys. Rev. B 37 (1988) 6113
- [38] M.D. Fleit and J.A. Fleck, J. Chem. Phys. 78 (1982) 301
- [39] R. Kosloff, J. Phys. Chem. 92 (1988) 2087
- [40] R.J. Taylor, Scattering Theory; the Quantum Theory of non-Relativistic Collisions (R.E. Krieger Publishing Company, Malabar, Florida, 1983)
- [41] E. Fattal, R. Baer and R. Kosloff, Phys. Rev. E 53 (1996) 1217
- [42] V. Kokoouline, O. Dulieu, R. Kosloff and F. Masnou-Seeuws, J. Chem. Phys. 110 (1999) 9865
- [43] R. Kosloff and D. Kosloff, J. Comp. Phys. 63 (1986) 363
- [44] D. Neuhauser and M Baer, J. Chem. Phys. 91 (1989) 4651
- [45] M. Maazouz, S. Ustaze, L. Guillemot and V.A. Esaulov, Surf. Sci. 409 (1998) 189
- [46] J.P. Gauyacq, A.G. Borisov, G. Raseev and A.K. Kazansky, Faraday Discussions 117 (2000) 15
- [47] J.J.C. Geerlings, J. Los, J.P. Gauyacq and N.M. Temme, Surf. Sci. 172 (1986) 257
- [48] J.N.M. van Wunnik, R. Brako, K. Makoshi and D.M. Newns, Surf. Sci. 126 (1983) 618

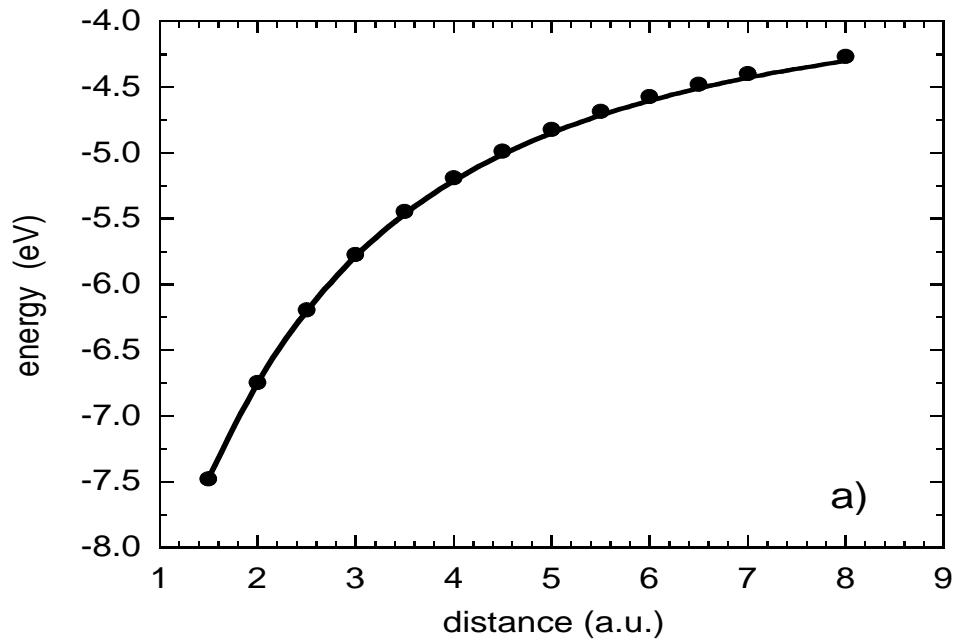


FIG. 1. Energy position of the F^- ion level in front of the $Al(111)$ free-electron-like surface, as functions of the ion-surface distance, measured from the image plane (atomic units). The solid line represents the results obtained with the present WPP approach. The black dots indicate the results obtained with the CAM method.

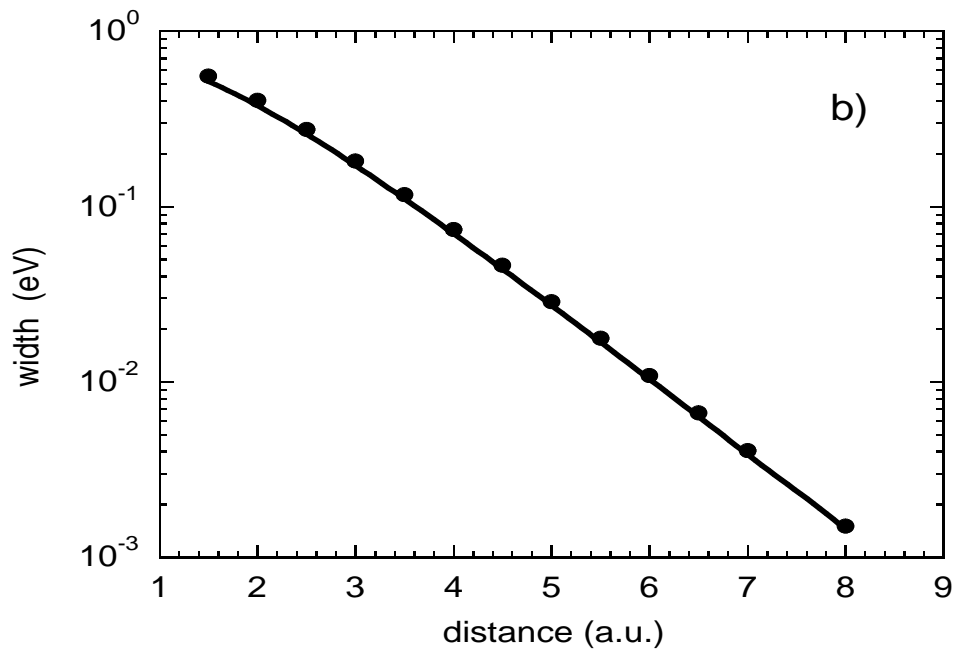


FIG. 2. Energy width for the same system as in Fig.1

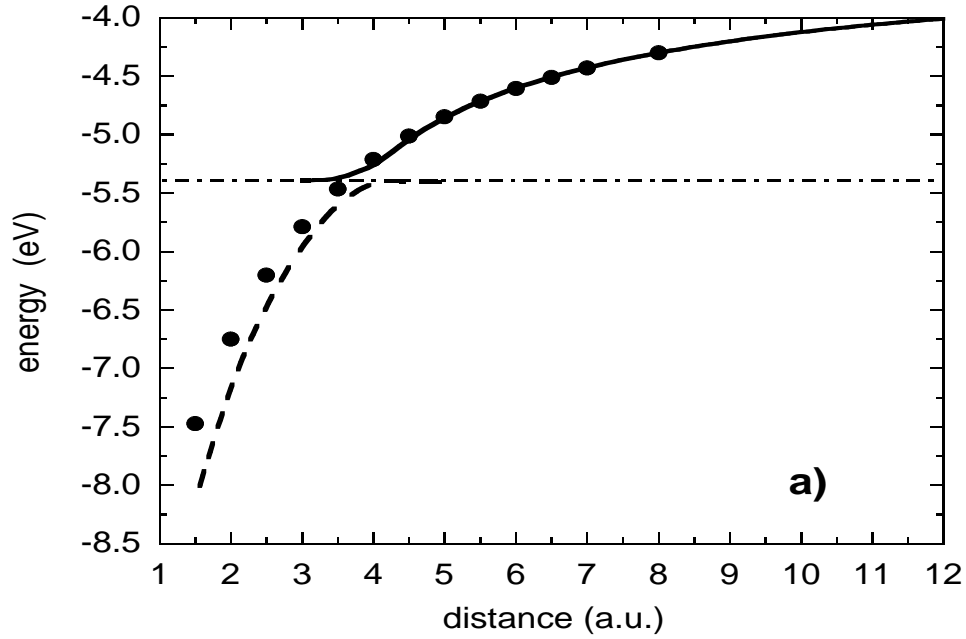


FIG. 3. Energy position of the F^- ion level in front of the model $Cu(111)$ surface, as functions of the ion-surface distance, measured from the image plane.(atomic units) The energy reference is the vacuum level. Black dots: results for the free-electron $Al(111)$ surface. The horizontal dashed-dotted line indicates the energy position of the bottom of the surface state continuum. Solid line: results for the highest lying resonance. Dashed line: results for the lowest lying resonance.

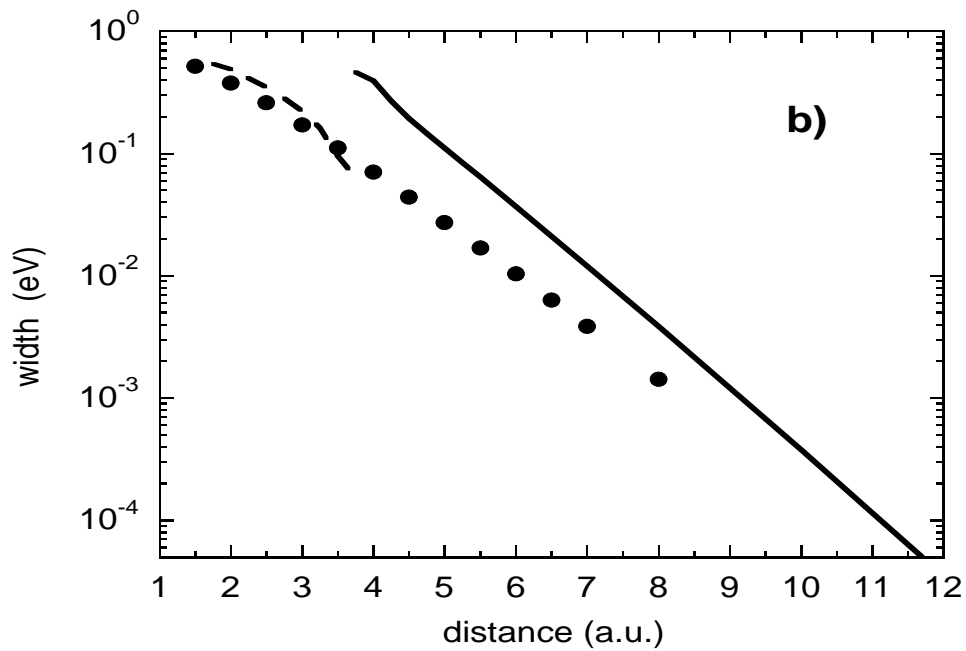


FIG. 4. Energy width for the same system as in Fig.3.

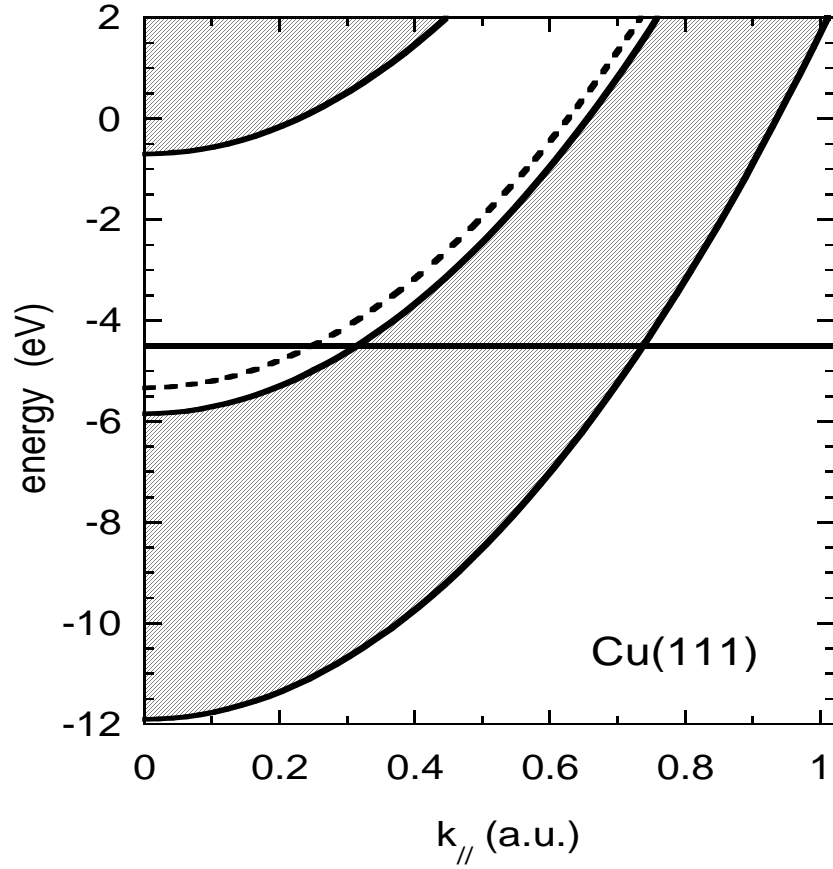


FIG. 5. A schematic picture of the electronic structure of $Cu(111)$ (work function 4.9 eV) as a function of the electron momentum parallel to the surface (atomic units). The energy reference is the vacuum level. The shaded area represents the 3D valence band continuum. The dashed line represents the 2D surface state continuum. The energy of F^- level at some distance from the surface is displayed as the horizontal solid line.

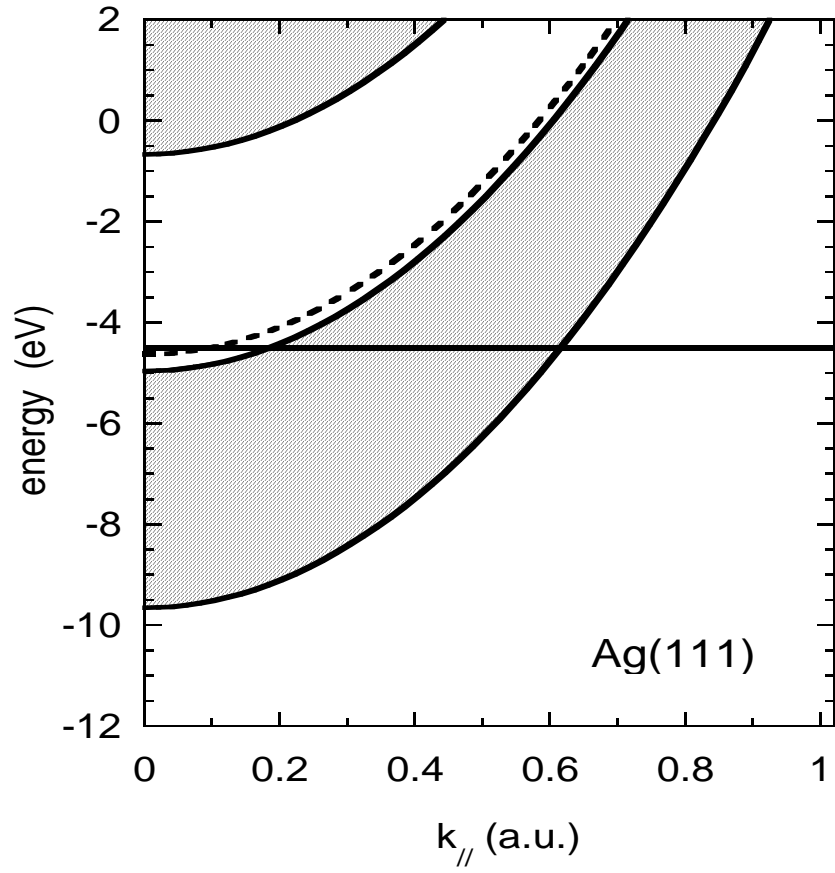


FIG. 6. Same as Fig. 5 for the *Ag*(111) surface (work function 4.56 eV).

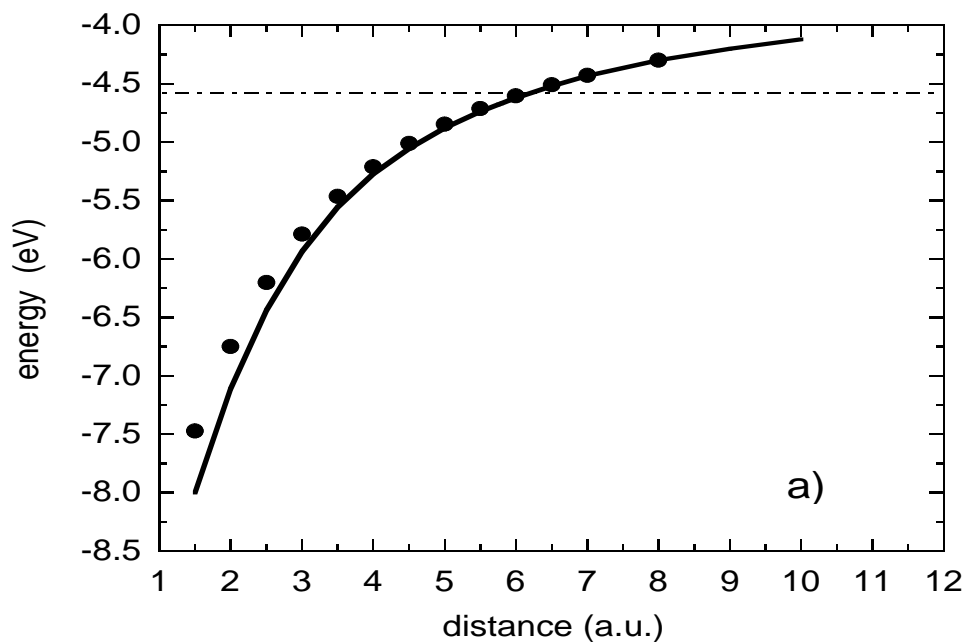


FIG. 7. Energy position of the F^- ion level in front of the model $Ag(111)$ surface (solid lines), as functions of the ion-surface distance, measured from the image plane (atomic units). Black dots represent the results obtained for the free-electron $Al(111)$ surface. The horizontal dashed-dotted line indicates the energy position of the bottom of the surface state continuum.

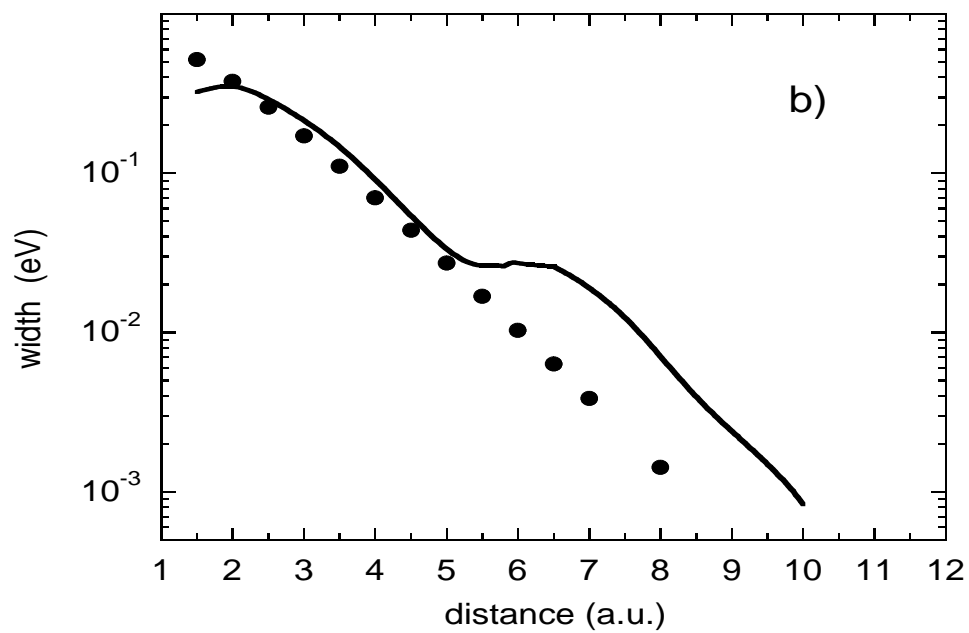


FIG. 8. Energy width for the same system as in Fig. 7.

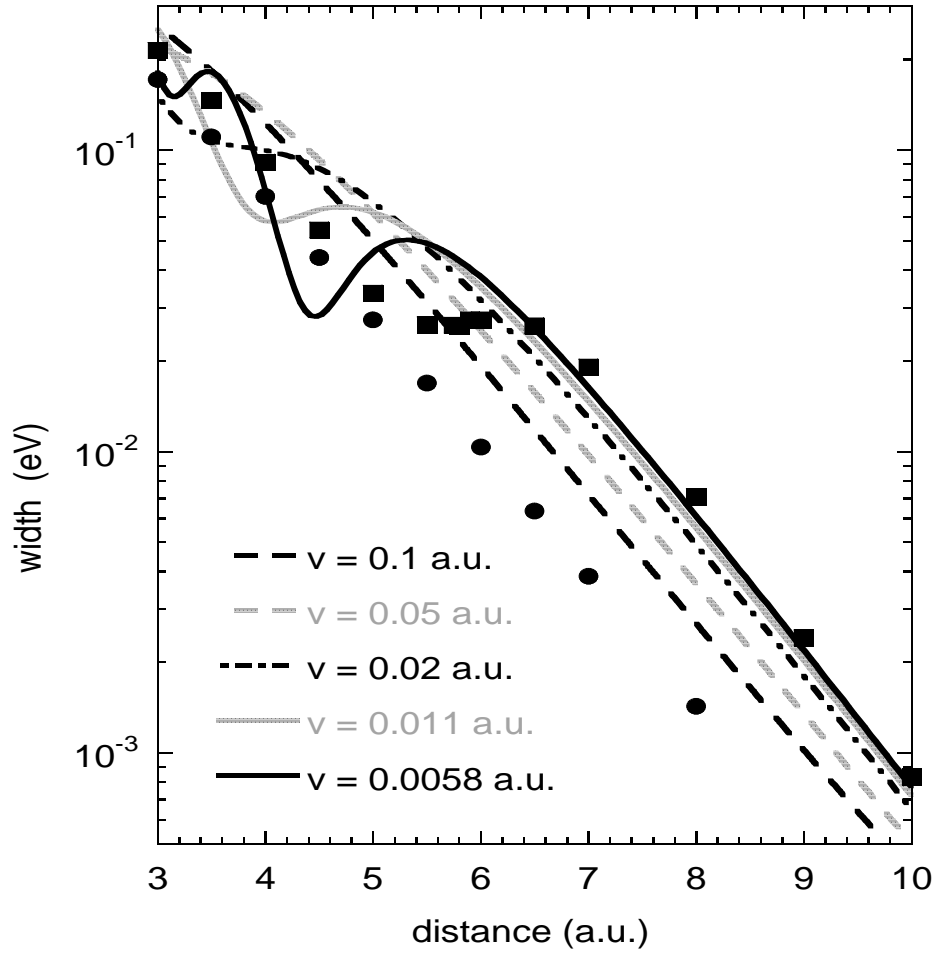


FIG. 9. The effective level width G versus the ion-surface distance Z for various collision velocities. The solid dots and solid squares stand for, respectively, the free electron and $Ag(111)$ static widths. Continuous lines represent the results obtained by the constrained wave packet propagation method for the model surface $Ag(111)$ for various collision velocities (see insert).